


Received September 1, 2019, accepted September 25, 2019, date of current version October 18, 2019.

Digital Object Identifier 10.1109/ACCESS.2019.2946191

# Performance Analysis of Disposable Flow Cell for Nitrite Detection

SABIRAN ABUBAKAR<sup>1</sup>, NORHANA ARSAD<sup>2</sup>, (Senior Member, IEEE),  
ABANG ANNUAR EHSAN<sup>3</sup>, (Member, IEEE),  
AZURA HAMZAH<sup>1</sup>, (Senior Member, IEEE),  
NUR HAZLIZA ARIFFIN<sup>4</sup>, AND  
MOHAMMAD SYUHAIMI AB-RAHMAN<sup>2</sup>

<sup>1</sup>Department of Electronic Systems Engineering, Malaysia-Japan International Institute of Technology, UTM, Kuala Lumpur 54100, Malaysia

<sup>2</sup>Center of Advanced Electronic and Communication Engineering, Faculty of Engineering and Built Environment, Universiti Kebangsaan Malaysia, Bangi 43600, Malaysia

<sup>3</sup>Institute of Microengineering and Nanoelectronics (IMEN), Universiti Kebangsaan Malaysia, Bangi 43600, Malaysia

<sup>4</sup>School of Engineering, Monash University Malaysia, Subang Jaya 47500, Malaysia

Corresponding author: Norhana Arsad (noa@ukm.edu.my)

This work was supported in part by the Ministry of Higher Education Malaysia and Universiti Kebangsaan Malaysia under Grant DIP-2018-017, and in part by the Faculty of Engineering and Built Environment, UKM, under Grant GUP-2019-010.

**ABSTRACT** This paper describes the work on the development of disposable micro sample cell for optical spectroscopy. The disposable flow cell is an attractive approach to ensure cleanliness of the sample container and to avoid contamination between samples and residual detergents. The main objective of this work is to develop a disposable flow cell made of Poly-(methyl methacrylate) (PMMA) with polymer optical fiber (POF) connections that is easy to install and has a performance measurement that meets ISO standards. The research involved three stages namely fiber optic preparation, design of the flow cell and analysis of the flow cell design. Chemometrics methods, internal quality control standards, calibration and performance characterization instruments are used for the analysis. The POF fiber performance is described by a linear calibration graph. The Shewhart chart for uncertainty analysis shows no data out of the chart, with mean value meeting the ISO 8258 standard. Comparisons of the calibration to other disposable sample cells show better results in linearity. Chemometrics analysis specified the reading data to be within the warning line in accordance with ISO 8258. Validation of the mathematical model is acceptable as none exceed 95% for the F-test. Average precision and sensitivity are 0.9 and 0.3, respectively. Limit of detection and limit of quantification are 0.07 and 0.25, respectively. Based on the results, the design of a disposable flow cell with POF fiber meets the standards of analysis for sample containers used in a spectrometer.

**INDEX TERMS** Absorption, control chart, ISO standard, polymers, sensors, spectroscopy.

## I. INTRODUCTION

Nitrites are chemical compounds that can cause environmental pollution [1] and have adverse effects on human health [2] besides imposing health risks on marine aquaculture [3].

Natural ground water resources are easily contaminated by this chemical compound [4], especially in ex-landfill sites [5] when microorganisms break down the nitrogen-containing organic compounds from animal manure, sewage waste, and plants [6]. The contaminated water will indeed have negative effects on living creatures, for example thwarting the growth performance of fish [7].

The associate editor coordinating the review of this manuscript and approving it for publication was Farid Boussaid.

Industrial sodium nitrite is commonly used as food preservatives. At high concentrations, these compounds have been known to incite cancer in a wide range of laboratory animals [8].

Spectrometers are well known instruments for detection and quantification of nitrite [9]. A fiber optic spectrometer is one of the methods used in a detection system [10].

The sample cell is the part that plays an important role in spectrometers because it is the place where interaction between light and sample occurs. There are two types of sample containers, which are the cuvette and flow cell. The advantage of the flow cell is that it can be used for continuous sampling to obtain data from the entire sample and provide realtime monitoring. The system is an essential tool

for quality monitoring process, such as realtime water quality monitoring [11].

However, most flow cells are either securely fixed during installation, nondisposable or fall short of being multipurpose. Hence, it is not suitable for continuous application due to residual from the solution or interference by the sample.

Disposable technology [12] in biopharmaceutical industry [13] manufacturing processes is significant such that it can increase efficiency by reducing capital costs [14], improve plant flexibility, reduce start-up time, and eliminate both non-value added process steps and the risk of cross-contamination. In addition, it also reduces labor costs in terms of liquid waste processing and on-site quality and validation requirements [15].

In this paper the development of a low-cost, robust, disposable flow cell coupled with POF spectroscopy for general application is presented. Nitrite is chosen study sample due to the harmful effects of the chemical compound and rapid growth in its detection systems.

This paper is organized as follows; Section II reviews the investigation on related works considered important in this study. Section III describes the methodologies applied for this project. Section IV shows POF performance and uncertainty analysis. Calibration and uncertainty analyses are presented in Section V. Chemometrics as statistical analysis is showed in Section VI, while Section VII presents characteristic performance of instruments and comparison among sample cells. The conclusion is presented in Section VIII.

## II. RELATED WORK

Various studies involving flow cells used as optical sensors in spectroscopy systems can be found in literature.

In [16], flow-injection spectrophotometry was developed for determining nitrite. The detection system was based on a diazotization reaction that traces amounts of nitrite in biological samples.

A patented design of an inline flow cell block with a flow passage of predetermined diameter was described in [17]. Interchange adapters were required for connecting the flow line of different internal diameters to the block.

A continuous flow was applied for a spectrometer to detect nitrite in water solutions [18]. To ensure gaseous products remain in the solution, high fluidic pressure was maintained throughout the experiment.

In [19], flow cell and spectrometer were established for nitrite detection in reagent concentration. A system injection was also applied for the system. Nitrate and nitrite in aqueous samples were determined with flow injection analysis [20]. The sample employed Griess reagent under acidic condition.

Spectrophotometric flow injection method was developed for nitrite or nitrate in soil samples [21]. The determination of nitrite was obtained by using a modified version of the Griess diazo-coupling reaction. Optical absorbance was observed at 543 nm.

A plastic disposable flow cell was applied in [22] for micro-array detection of infectious agents for clinical

laboratory. In [23], the application of polyethylene flow cell for chemical detection with POF was developed based on absorbance spectrophotometric method and the simple design flow injection made of PMMA acrylic for nitrite determination was showed in [24].

As observed from the literature study, various flow cells are implemented for nitrite detection. However, there is still a need for a design that is guided by the “simpler, cheaper and smaller” principle, with more focus on continuous flow and the demand for mechanical resistance and better robustness [25].

## III. METHODOLOGY

Three steps were involved in designing the proposed disposable flow cell, which are the fiber optic preparation, design of the flow cell, and analysis of the design.

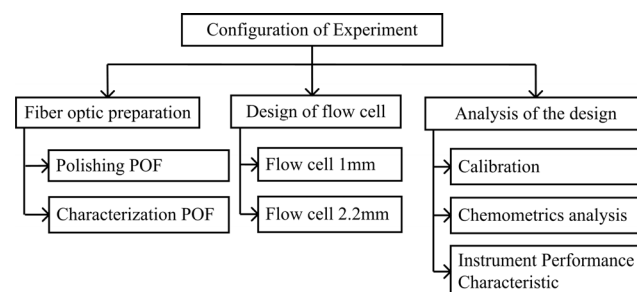


FIGURE 1. Scope chart of the experiment.

In the design, an approach was taken to validate the design of disposable sample cells by using data comparison with the conventional disposable sample cells, a cuvette. Both methods of using flow cells and cuvettes were applied to a fiber optic spectrophotometer. POF was chosen for the fiber optic component due to its large numerical aperture, which allows optimum interaction between the light signal and the sample.

### A. FIBER OPTIC PREPARATION

In this work, the POF with 1 mm core diameter (ESKA™SH 4001-1.3, Mitsubishi Rayon Company Ltd.) was used. The core of the POF is made of PMMA, which coated by fluorinated polymer and enclosed by polyethylene jacket. The connector used for the POF is SMA 905 which is manufactured by Industrial Fiber Optics.

The POF needs to be prepared prior to usage. The complete preparation steps of the POF and SMA connector are shown in Figure 2. Firstly, the fiber was cut using a fiber cutter as shown in Figure 2(a). Secondly, the jacket with 16 mm length was stripped from the POF by using a clipper (Figure 2(b)). Then, the bare fiber was inserted into the ferrule of the connector as shown in Figure 2(c). Next, the connector was crimped using a crimping tool as shown in Figure 2(d). Finally, the glue was inserted in between the connector and the POF. This was to avoid any leakage to occur between the connector and the metal hoop during the experiment.

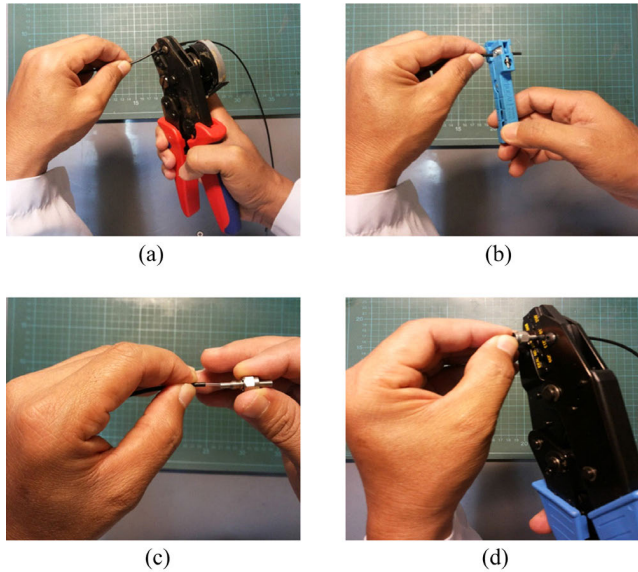


**FIGURE 2.** Preparation process of POF and SMA connectors. (a) POF fiber cutting (b) POF jacket removing (c) SMA connector installing (d) Crimping of fiber connectors.

1) POLISHING POF

There were two steps for polishing POF, namely rough level and fine level polishing. The rough stages were done manually on dry sandpaper whereas the smooth stages were done using a polishing machine, ULTRAPOL Fiber lensing machine. The machine produced accurate profile of the fiber. In this polishing machine, water was used to remove residual dust produced during the polishing process.

Figure 3 shows two steps of polishing. The first polishing step was done using a POF fiber-optic kit angle of 90° and in a figure-eight motion onto sandpapers with roughness of 10 μm and 3 μm. Sandpaper with 10 μm roughness was used to eliminate the excess POF core from the ferrule of the SMA connector. Sandpaper with 3 μm roughness was used for smoothing the end of the connector.



**FIGURE 3.** Steps of polishing process (a) first stage: manual, dry polishing (b) second stage: using polishing machine, wet polishing.

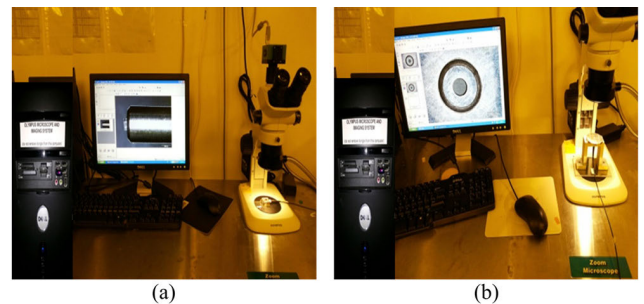
The second step of polishing was carried out by using a polishing machine. This step is carried out to get better result of smoothing and to clean up the surface of the fiber core.

The machine utilized aluminum oxide polishing paper with roughness of 0.5 μm and 0.3 μm. Water jet was applied to remove the dust away.

2) POF CHARACTERAZATION

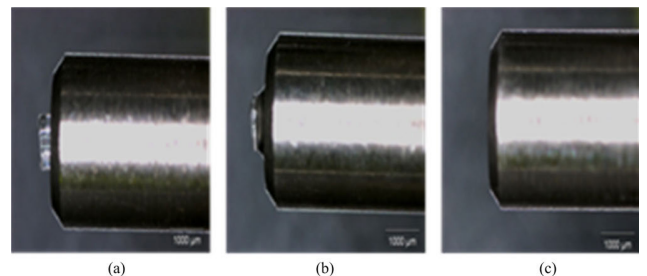
POF connector characterization was done using stereo zoom microscopes by OLYMPUS type SZ51. The optical fiber’s surface image was acquired from manual inspection through the eyepiece, whereby images were captured and displayed on a computer screen via USB cable.

Figure 4 shows the configuration of POF characterization. Figure 4 (a) shows the set-up for edge connector characterization and Figure 4 (b) shows the set-up of surface of POF.



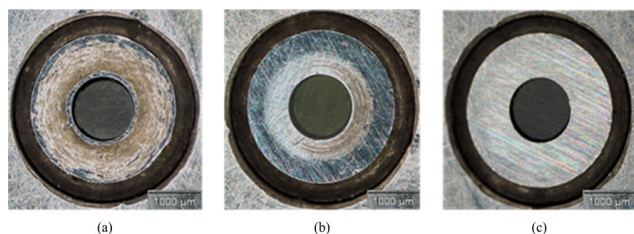
**FIGURE 4.** Microscope configuration for POF characterization (a) edge of the connector, and (b) surface of the connector.

Figure 5 shows the edge of connector’s ferrule and fiber core obtained from the microscope, while Figure 5 (a) shows the image when the POF was inserted into the metal hoop of SMA connector. The tip of POF was slightly oriented outward from the ferrule about 20 μm. This size depended on the accuracy of the installation and size of uncladded fiber jacket. The gap between the core of the fiber and the midline of the ferrule was filled in with epoxy glue as shown in Figure 5 (b). This gap should be small enough to prevent the sample from being drained when applied to the flow cell. Figure 5 (c) shows the manually polished ferrule using 10 μm papers. The end of the fiber was found flattened and eroded. However, additional polishing was required for smoothing was obtained by using finer polishing paper.



**FIGURE 5.** Image of POF characterization (a) POF fiber position, (b) epoxy glue effect on the connector, (c) polishing with sandpaper 10 μm.

The image of surface characterization is shown in Figure 6. This figure shows the polishing result of the tip of the POF



**FIGURE 6.** Image of surface characterization POF; (a) Manual polishing with sandpaper 3  $\mu\text{m}$ , (b) Polishing machine with polishing paper 0.5  $\mu\text{m}$ , (c) polishing machine with sandpaper 0.3  $\mu\text{m}$ .

surface. Figure 6 (a) shows the result of manual polishing with 3- $\mu\text{m}$  sandpaper roughness. There were scratch marks appearing on the surface the POF. These marks could cause refraction and scattering of the rays that propagate through the fiber, thus reducing the optimum light that reaches the sample cell.

Polishing with fine grade polishing paper was aimed to reduce surface scratches. For this step, a polishing machine was utilized. The machine provided spin stability, a water jet for removing residual dust, and controlled pressure onto the sandpaper. Employing the polishing machine indeed provided better surface results. The water flow during polishing process was to remove excess dust as a result of polishing.

The polishing results from using sandpaper of roughness 0.5  $\mu\text{m}$  is shown in Figure 6 (b). Figure 6 (c) shows a better result obtained from polishing on a graded sandpaper of 0.3  $\mu\text{m}$ . Finer and flatter POF core surface conditions were required to reduce the impact of refraction and scattering of light thus making the light propagation within the POF core more optimal.

### B. DESIGN OF FLOW CELL AND CASING

Figure 7 shows the design and picture of the flow cell. Figure 7 (a) and (b) show 3D design of 1 mm and 2.2 mm of flow cell.

The flow cell was made of PMMA polymers with thickness of 10 mm. The casing was made of 1 mm thickness aluminum.

A photograph of the casing is shown in Figure 7 (b), while the photograph of the casing and the flow cell is shown in Figure 7 (c).

Size of the casing was 24 mm in length and 21 mm in width, whereas the flow cell was 22.2 mm in length and 19 mm in width. The 6.3 mm diameter hole in the casing had a slot for the SMA plug. This adapter connector was used to insert the sample through the appropriate syringe, which was then used for sample injection.

The casing was attached to a hook to hold and ensure the configuration was rigid throughout the measurement, sample flow and the sample cell replacement processes.

### C. MEASUREMENT INSTRUMENT

Basically, there are three main elements for absorption spectrophotometry measurement, namely light source,

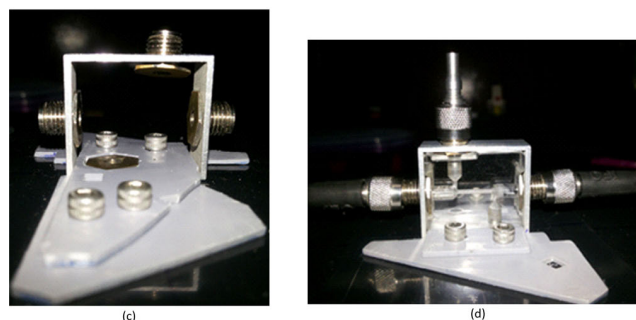
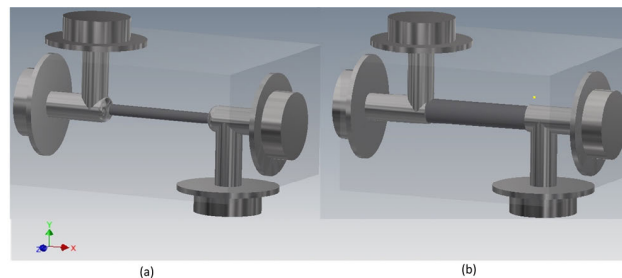


**FIGURE 7.** Design of flow cell and casing; (a) 3D design of 1 mm flow cell, (b) 3D design of 2.2 mm flow cell. (c) Casing photograph without flow cell, (d) Photograph of casing, flow cell, and SMA connector.

spectrophotometer, and software for obtaining data. Optical fibers and sample containers are additional elements.

In this study, the light source is the DH-2000-BAL balanced deuterium halogen light manufactured by OceanOptic<sup>TM</sup>. This light source uses innovative filtration technology to produce a smooth spectrum across the entire range of the spectrum. This technology eliminates the alpha line between the deuterium in the visible light ray region. The wavelengths within the range of ultra-violet to near infrared are between 200 nm to 1100 nm.

To measure and analyze the spectrum, OceanOptic<sup>TM</sup>'s HR4000CG-UV-NIR spectrophotometer is used (*High Resolution - Composite Grating Ultraviolet - Near Infra-Red*).

### D. SAMPLE PREPARATION

The sample consists of two types, namely nitrite and Greiss reagent samples. The Greiss reagent is the chemical reagent used to detect the presence of nitrite organic compounds. The presence of nitrite is determined based on the appearance of pinkish gradation when the reagents were mixed.

Samples and reagents were in the form of solids, while nitrite and sulfanilamide were in the form of salts. Additionally, N-(1-Naphthyl) ethylenediamine hydrochloride was in powder form. The sample in this reagent was then dissolved in standard deionized water to obtain a solution of a certain concentration.

Molarity concentration is applied to calculate the sample concentration. Nitrite solution was prepared by diluting 0.0138 g of sodium nitrite in 200 mL of water. The concentration of the solution is decreased to 6.9 ppm of 1 mL volume by diluting 0.1 mL into 0.9 mL of deionized water. Furthermore, by diluting the 2 mL of the concentration into 2 mL will be resulted 0.345 ppm.

Six sample concentrations were prepared and used in this study; 3.450 ppm, 1.725 ppm, 0.863 ppm, 0.431 ppm, 0.216 ppm, and 0.108 ppm. Total volume of the sample is 260 mL. It's no effect of environment due to the small amount.

### E. CONFIGURATION OF EXPERIMENT

The design and photograph of the flow cell in this study are shown in Figure 8. Figure 8 (a) describes the experiment setup including light source, spectrometer, data acquisition, and apparatus. The experiment was carried out at room temperature by using a stop flow method.

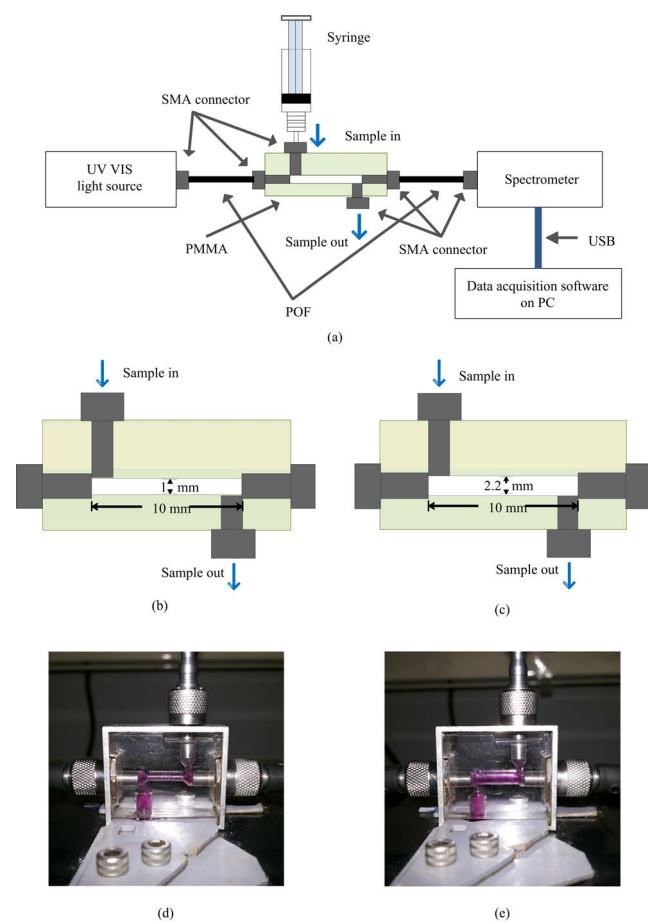


**FIGURE 8.** Configuration of the designed flow cell; (a) detailed design, (b) flow details of 1 mm stream, (c) flow cell details of 2.2 mm flow cell, (d) photograph of 1 mm flow cell, (e) photograph of 2.2 mm flow cell.

The design input and output of the sample into the light path length with two 1 mm diameter sizes are shown in Figure 8 (b) and flow cell 2.2 mm, in Figure 8 (c). Figure 8 (c) and (d) shows the photograph of the flow cell. This design enhanced the robustness and stability of the sample cell by having a compact casing connected to the SMA connectors.

The designs produced flow cell volumes of  $7.85 \mu\text{L}$  and  $38 \mu\text{L}$  for diameter of 1 mm and 2.2 mm, respectively.

The determination of the flow cell diameter size was based on the size of POF core diameter and jacket diameter.

The spectrometer was placed in a stable position and locked with a screw to ensure a fixed position and prevent any vibrations that might cause the grating to shift and thereby result in errors during the light spectrum reading.

Photographs of the experimental setup are shown in Figure 9, where Figure 9 (a) presents the configuration for the cuvette while Figure 9 (b), for the flow cell. The PMMA semi-micro disposable cuvette is used in the experiment, with 10 mm path length, and 1.5 mL volume. The cuvette is chosen for comparison due to the similarity of material, path length, and disposable capability.

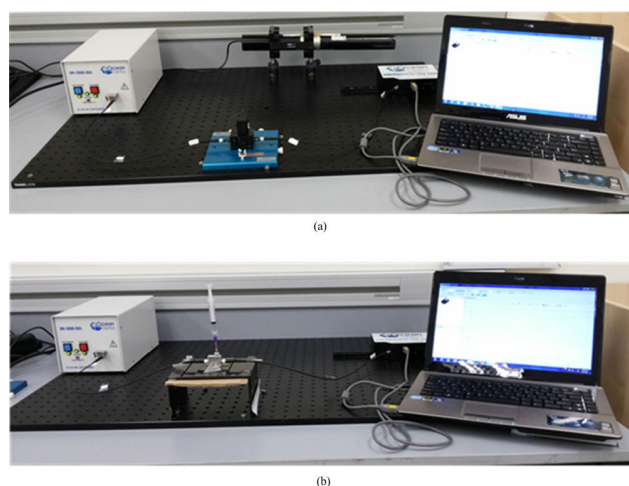


**FIGURE 9.** Experiment configuration for sample cell (a) cuvette, and (b) flow cell.

### F. MEASUREMENT PROCESS

Light spectrum absorption measurement of samples using disposable sample cell is the goal of this study. In order to achieve this goal, three experiments were performed including the experiment on POF performance, comparing sample cuvette and flow cell.

Flow chart in Figure 10 is used to describe the measurement process.

The steps of preparing the experiment configuration, the process of arranging for data acquisition and the measurement of the light spectrum from the sample are as shown in the flow chart. The experiment is run in room temperature and stop flow methods.

In nutshell, there were three steps of the measurement, which include preparing light source, storing reference and absorbance spectrum measurement.

As using greiss reagent method for the sample, standard peak absorption is at 543 nm. The spectrum was not displayed since focus this study on analysis instrument.

Data spectrum was stored in 20 seconds intervals for 4 minutes. Hence, 12 sets of spectra data for each sample were obtained. These data were needed for chemometric or statistical analysis.

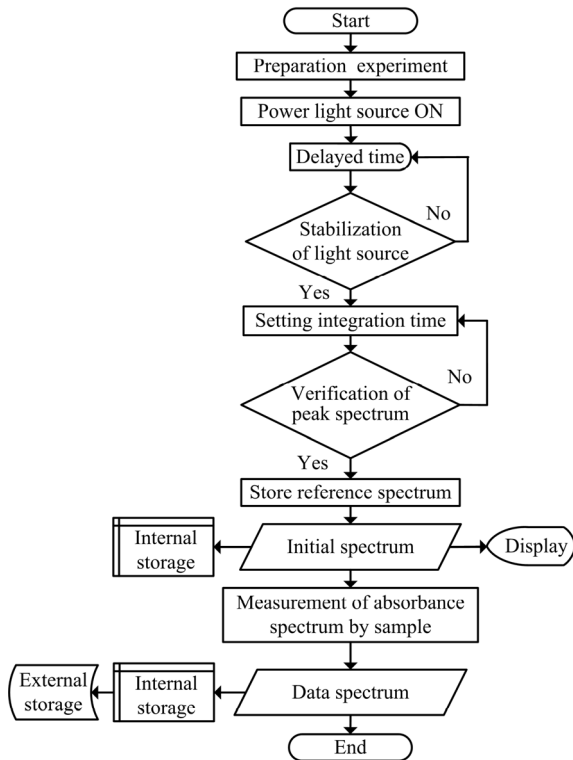


FIGURE 10. Flow chart for general measurement process.

#### IV. POF PERFORMANCE ANALYSIS

Calibration analysis was performed to identify the performance of POF that was used directly (without lens collimator) based on an extrinsic detection approach.

Calibration is defined as a comparison between data measurements or correctness made or set with one device data that acquired by calculation in linear system [26]. In this work, the partial least square regression method was applied to define the true absorbance, as shown in equation (1):

$$y = mx + b \quad (1)$$

The calibration data was obtained from absorption of light to sample. The spectrums of the absorption were plotted as actual absorbance on a regression calibration graph, Fig. 11. Hence, true absorbance is prediction of linearity line of the peak absorbance data.

The peak of optical absorption of the spectrums was at 453nm since the samples were greiss reagent compound, the In this study magnitude of the spectrum is shown in point calibration graphs not separated graphs due to focus instrument analysis on analysis not chemical compound analysis.

The calibration response of the POF is shown in Figure 11. The graph was generated through a LINEST function as suggested by [27] based on calculations using regression from a spreadsheet program. The function is based on equations (2), (3) and (4).

Warning line is defined as:

$$\bar{x} \pm 2s \quad (2)$$

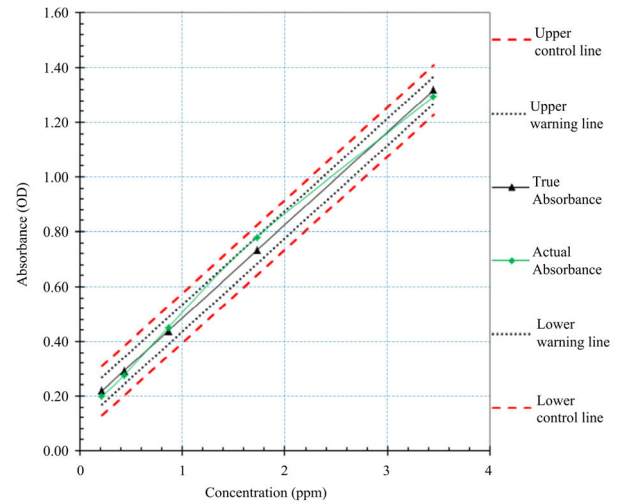


FIGURE 11. Calibration plot and uncertainty analysis.

Control line is defined as:

$$\bar{x} \pm 3s \quad (3)$$

$S$  standard deviation:

$$s = \sqrt{\frac{\sum_{i=1}^N (x_i - \bar{x})^2}{n - 1}} \quad (4)$$

where  $\bar{x}$  is average for each spectrum data,  $s$  is standard deviation and  $n$  is number of measurement.

Data control analysis was used to identify data qualification for internal quality control (IQC). The IQC is fundamental for analytical quality assurance (AQA) [28]. The analysis applied the Shewhart chart, which is a control chart to determine the characterization of measurement data. This data characterization was based on ISO 8258, where at least ten data readings were required for each measurement [29].

In this analysis, an uncertainty limit is given where the instrument signal response for each sample concentration and the confidence level of the data obtained. The uncertainty shown in a confidence interval is uncertainty estimation.

In this analysis, interval of uncertainty was shown in warning line and control line. The line were indicated confident level of the measurements. The confident level of 95% and 99% were stated in between warning line and control line, respectively.

The actual absorbance is spectrum absorption of each sample that was displayed in the instrument. The true absorbance is defined through calculations. Instrument readings were within the warning line, which meant that the maximum error rate for a one-tail test was 2.5%.

The graph indicates that the absorption of light is directly proportional to the concentration and is within the range of confidence limits on the lower and lower limit lines.

**V. COMPARISON OF CALIBRATION**

Comparison of calibration is shown in Figure 12. The comparison was between the 1 mm diameter flow cell, a 2.2 mm diameter flow cell and a cuvette with a POF connector.

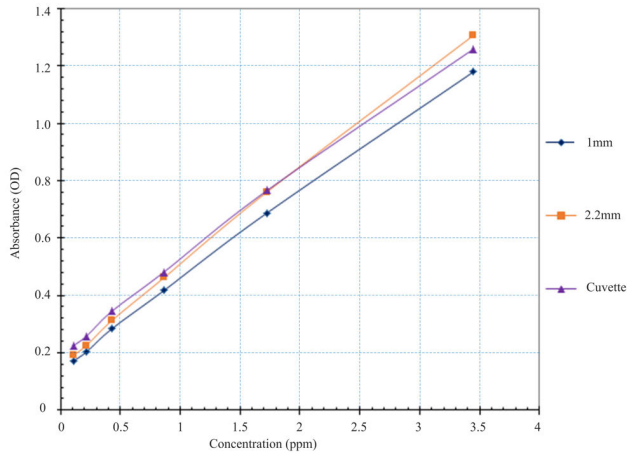


**FIGURE 12. Calibration curve of flow cell and cuvette.**

The characterization of light absorption values showed the same pattern of absorption rate to the concentration of all sample containers but with a slight difference in 3.45 ppm concentrations, i.e., 1.180, 1.31, and 1.26 for 1 mm, 2.2 mm, and cuvette, respectively.

The cuvette absorption value was higher at the concentration of 0.108 ppm, 0.122 ppm, 0.431 ppm, and 0.863 ppm compared to the 1 and 2.2 mm flow cells. At a concentration of 1.725 ppm, the value absorption of the cuvette is equal to the value of the flow cell up to 2.2 mm. However, the at highest sample concentration of 3.45 ppm concentration, its absorption values are lower than 2.2 mm flow cell but still higher than 1 mm flow cell.

It occurred at the highest concentration only. The phenomenon is caused by the volume and concentration effect of the sample.

The linearity line of the flow cell is indeed better than the cuvette. This was due to geometrical effect of the sample cell, where cylinder form showed less diffraction of light. A study by [30] confirmed the phenomena.

Though its absorption value for each concentration is lower than the other sample cells, the calibration curve pattern of the 1 mm flow cell is still better in terms of linearity.

**A. REGRESSION AND CORRELATION**

Detailed analysis of the calibration were accomplished using regression and correlation methods. The LINEST function [27] and linear regression were applied in the analysis as follows:

The parameters in Table 1 are slope of the line (m), y-intercept of the line and correlation. The highest value of the slope is obtained from the 2.2 mm flow cell whereas the lowest is the 1 mm flow cell. The cuvette shows the highest y-intercept value while the lowest is given by the 1 mm

**TABLE 1. Regression and correlation.**

Parameters	Flow cell		Cuvette
	1 mm	2.2 mm	
Slope (m)	0.3019	0.3342	0.3099
Intercept (b)	0.1490	0.1652	0.2053
Correlation (R <sup>2</sup> )	0.9992	0.9991	0.9982

flow cell. Moreover, with respect to correlation parameters, the highest value comes from the 1-mm flow cell, whereas the lowest is the cuvette.

Regression analysis and correlation both show that the 1 mm flow cell has better features and capabilities than the other sample cells. In addition, the data of the entire sample cell fulfilled the criteria of standard calibration.

**VI. CHEMOMETRICS ANALYSIS**

Chemometrics is the science of extracting chemical data information in which it uses mathematics, statistic and formal logic [31]. This analysis is deemed to be the best approach to avoid misinterpretation of large amounts of complex analytical chemistry data [32].

Data quality control, mathematical validation, and normal distribution were the techniques applied in this study.

**A. DATA QUALITY CONTROL**

A box plot graph was used to describe the comparison of data quality control. The graph presents a data summary from all the data of the entire sample concentrations and sample cells that were being studied in this project.

The charts were plotted by using equations (2) and (3). Furthermore, this chart shows parts of a Shewhart data control analysis, the target value, the data above the upper data, the data below the lower data, the warning line, and control line. The warning lines are data limits that fall within the control area before the action line. If the data fluctuates over and out of the action line, then the data will not be accepted and considered as an error.

The box plot illustrates higher than average and below average data values in different colors, while average values are illustrated by lines within the box, in between the two colors. The warning line is indicated by the black line range while the action line is indicated by the red line range.

This study applied two types of data control; average value control and data range control.

**1) AVERAGE VALUE CONTROL**

A summary of the average quality data from the overall measurement data is shown in Figure 13.

The chart shows that there were no average value data beyond the upper and lower limits. Some data were located at the center of the target line 0.00; i.e. at concentration of 0.108 ppm for the 2.2 mm flow cell and cuvette; at a concentration of 0.863 ppm and 1.725 ppm for the 1 mm flow cell.

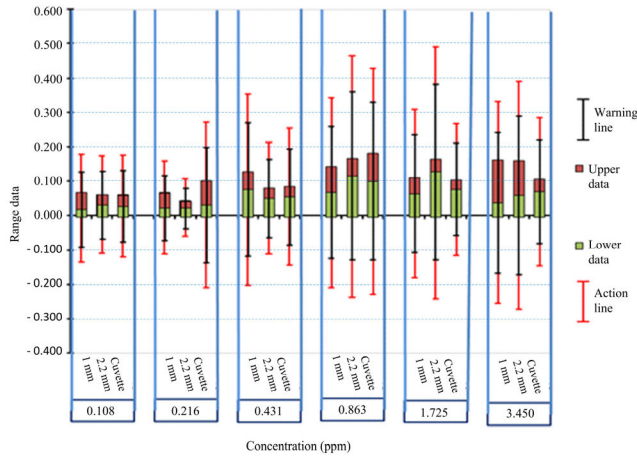


FIGURE 13. Box plot chart for average value.

This indicates that the average value is in control and data fluctuation is still within the warning area.

At a concentration of 0.863 ppm, cuvette exhibits the highest data volatility whereas at concentration of 0.216 ppm the lowest data fluctuation were obtained for 2.2 mm flow. Data downgrades did not shift away from the warning line, which meant that all data achieved IQC. This fulfilled the ISO 8258 standard.

2) DATA RANGE CONTROL

The control of the data range illustrates the variability of a measurement process. Figure 14 shows the control of data range in a plot box chart. In general, the measurement range is lower than the warning line and control line. The small differences caused some data above the average line and below the average line to be undetected.

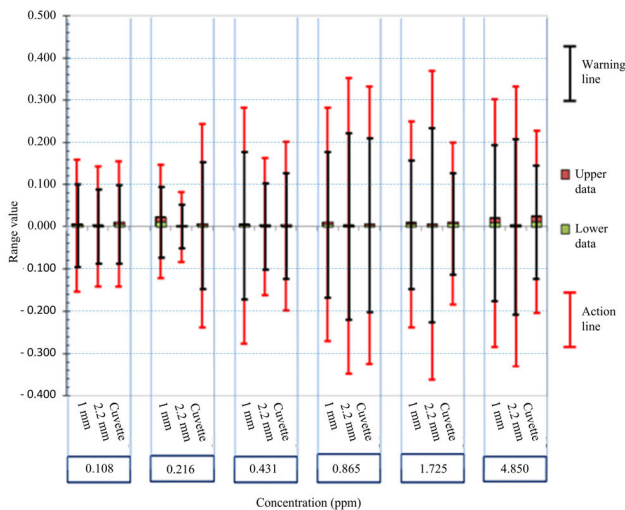


FIGURE 14. Box plot chart for data range.

Warning lines and control lines are larger than the data fluctuation range. This proved that the variation of data range

is small and the measurement data is good, hence the range of data meets the IQC standards.

The measurement of data range for all data is less than 0.02 which indicates minimum data fluctuations. However, there were three ranges approaching 0.05, at concentrations of 0.216 ppm and 3.450 ppm for a 1 mm flow cell and at concentration of 3.450 ppm for the cuvette. Only three of these data clearly show the data in the area above and below the target line. According to ISO 8258, the data met the standards.

B. VALIDATION OF THE MATHEMATICAL MODEL

Validation of the regression model is needed to confirm that the chosen model adequately describes the relationship between variable *x* and variable *y*. Confirmation was needed to verify that the model can be best described as a straight line or whether the data is better described as a curve [33].

The validation model was performed in two steps using residual regression and  $\hat{F}$  test.

Residual regression:

$$e_i = \bar{y}_i - y_i \tag{5}$$

The residual regression is a differential value between calculated linear line and actual value of absorption shown by the instrument. The residual regression as shown in Figure 15 was calculated by using equation (5) and the absorption value was as shown by the instrument. The residual value will be positive if the actual value is lower than the value of the instrument reading and vice versa.

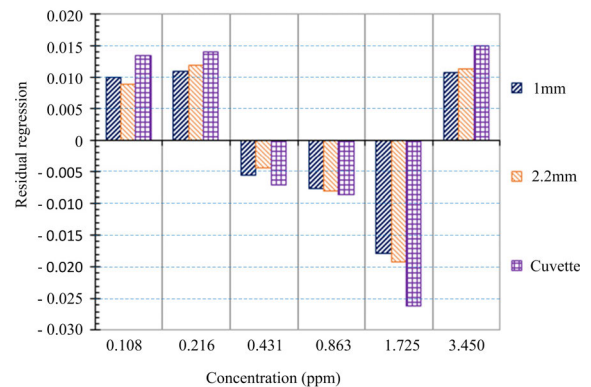


FIGURE 15. Residual regression.

In general, residual regressions of the cuvette are higher than the other two flow cells. This shows that the error obtained from the cuvette is greater than the 1-mm and 2.2 mm flow cells. The error pattern for the three sample containers was the same but the regression residual values of the three sample containers were different. At a concentration of 1.725 ppm, the regression tray exhibits the highest value which occurs for all sample cells.

The second validation of the mathematical model was determined by comparing value of  $\hat{F}$  from equation (6) to  $\hat{F}$  distribution table in appendix. The  $\hat{F}$  distribution table



consists of two decisive significance P, i.e., at P 99% and P 95%. Data is considered valid when the value of  $\hat{F}$  is lower than the F distribution table.

$\hat{F}$  test:

$$\hat{F} = \frac{(n - 2) \cdot s_{y,x}^2 - (n - 3) \cdot s_{y,x,OL}^2}{s_{y,x,OL}^2} \quad (6)$$

A comparison of  $\hat{F}$  to the  $F$  in table F is shown in Figure 16. The  $\hat{F}$  value for all samples did not exceed the significant level of P 95%; this meant that the validation of the mathematical model for this regression is acceptable at 95%. The  $\hat{F}$  values were 3.676, 4.226 and 4.715 for the sample cells of the 1 mm flow cell, 2.2 mm flow cell and cuvette, respectively.

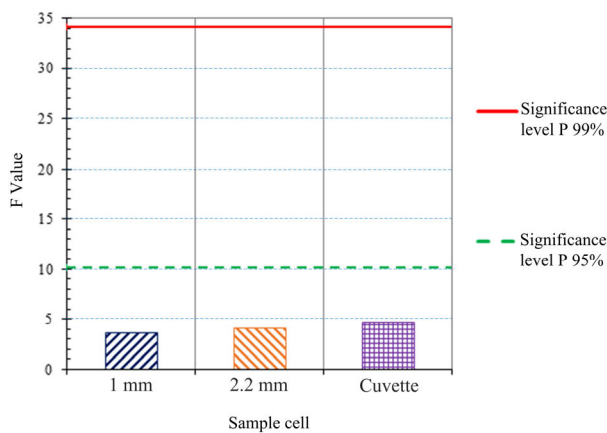


FIGURE 16. F-test for validation of the mathematical model.

### VII. PERFORMANCE CHARACTERISTICS OF INSTRUMENT

The quantitative instrument performance criteria were used to decide whether the instrument method was suitable for analytical analysis. These characteristics were expressed in numerical terms known as figures of merit [34]. In this study the criteria of analysis were precision, accuracy, sensitivity, limit of detection and quantitation, and dynamic range [35].

#### A. PRECISION

Precision of a measurement is defined as closeness of agreement between independent test results obtained under a stipulated condition. It is a crucial performance characteristic in analytical chemistry [36].

Data acquisition from instrumental analysis was repeated for more than ten times to achieve stability and homogeneity. Precision was made by determining the level of readability of each recurrence measurement. As shown in equation (7) and (8), numerical values of precision increases with a decrease in error. The normal range was from 1 to 0; for a dispersion-free measurement the precision becomes 1. On the other hand, the precision becomes 0 if dispersion amount to standard readings or standard deviation (*rsd*) becomes 1 or 100%. Therefore, high precision is characterized by a high value of precision. The precision becomes negative if the

error exceeds the measured value of *rsd* more than 100%. But this particular case rarely occurs in analytical chemistry [37].

In analytical science, there are usually two types of precision, namely the procedure and the result of the analysis. In this study, both the precisions were examined.

#### 1) PRECISION OF AN ANALYTICAL PROCEDURE

The precision of analytical procedure can be calculated by subtracting the relative standard deviation from 1 as follows:

$$prec(x) = 1 - rsd(x) \quad (7)$$

Figure 17 shows the precision of the procedure of 1 mm flow cell, 2.2 mm flow cell, and cuvette. The lowest precision was 0.945 at concentration of 1.725 ppm for the 2.2 mm flow cell. The highest precision was 0.988 at 0.216 ppm for a 2.2 mm flow cell. The other precisions of the concentrations are between them.

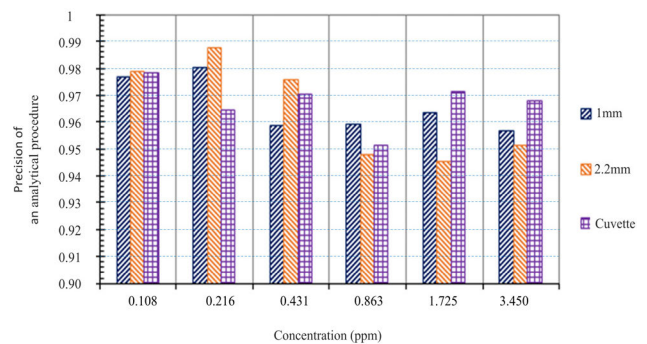


FIGURE 17. Precision of an analytical procedure.

In general, the precision were 0.966, 0.964, and 0.967 for 1 mm flow cell, 2.2 mm flow cell, and cuvette, respectively. In general, the precision of the sample cell was 0.9 and met the precision standards of the procedure; the highest value is 1 while the lowest value is 0.

#### 2) PRECISION OF AN ANALYTICAL RESULT

The quantification of precision of an analytical result can be defined by means of relative confident intervals as follow:

$$prec(\bar{x}) = 1 - \frac{\Delta\bar{x}}{\bar{x}} \quad (8)$$

The precision of analytical result is shown in Figure 18 The figure illustrates the analysis for each sample concentration in various sample cells. The precision of analytical value was in the range of 0.5 to 1, the lowest value being 0.563 at 0.431 ppm concentration for 1 mm flow cell, while the highest precision was 0.917 at 3.450 ppm concentration for the cuvette.

A study of precision is influenced by the stability of the sample cell position. This was evident from the lower precision value of the 1 mm flow cell than the 2.2 mm flow cell. The POF core acting as the connector of light rays from the light source to the spectrometer has the same diameter with that the 1 mm flow cell. If there were any small misalignments

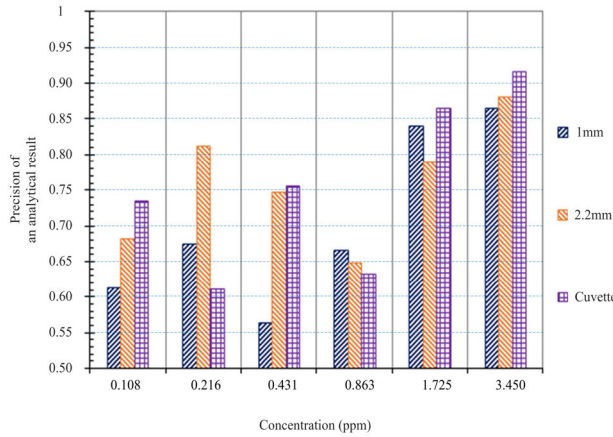


FIGURE 18. Precision of an analytical result.

between the core and the sample cell, some of the light would be scattered and bounced out. This would result in attenuated precision due to loss of ray power.

However for the 2.2 mm flow cell, the diameter was larger than the POF size. Hence, the misalignment problem between the POF core and the sample cell was minimized. Therefore, the probability of scattered and reflected light was kept minimum thus improving precision.

In general, the precision values were 0.704, 0.760, and 0.753 respectively for 1.0 mm flow cell, 2.2 mm flow cell, and cuvette. In a nutshell, the precisions for the three samples were 0.7, which met the precision of analytical standards; the highest value being 1, while the lowest is 0.

**B. ACCURACY**

The data obtained from an analytical instrument should not have a significant deviation from the actual value based on the calculation of the calibration chart. The accuracy study consists of two type of investigations, namely systematic error and accuracy. Systematic error is used to obtain the calibration error percentage level while accuracy is shown in the maximum range of 1.

Systematic errors displace the individual results of measurement one-sided to higher or lower values, thus leading to incorrect results. The existence and magnitude of systematic errors are characterized by the bias. The bias of a measured result is defined as a consistent difference between the measured value  $y_{test}$  and the true value  $y_{true}$  [36].

$$bias(y) = y_{test} - y_{true} \tag{9}$$

Based on equation (9) systematic error is obtained as showed in Figure 19. Error value is positive if the test value is greater than true value, otherwise the error value is negative. Negative and positive errors occurred at the same concentration for each sample cell, although the range of values is different.

The number of positive errors (within the range of calibration limits) occurred at three concentrations, i.e. 0.431 ppm,

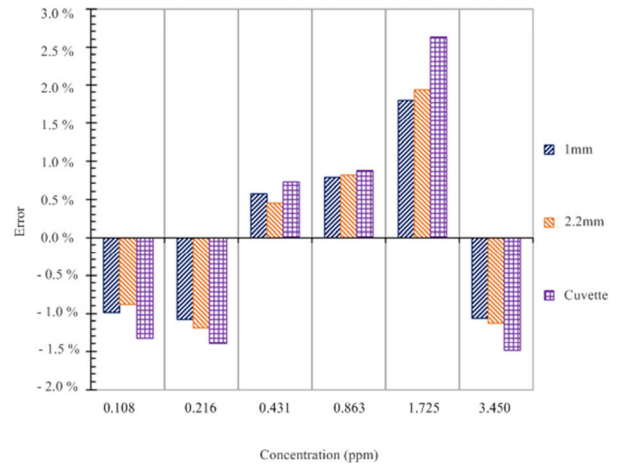


FIGURE 19. Systematic error.

0.863 ppm, and 1.725 ppm while the negative errors occurred at 0.108 ppm, 0.216 ppm, and 3.450 ppm. Positive or negative values occur due to fluctuations in light. This value of fluctuation is less than 5%. If more, then the linearity will decrease.

The biggest error value was 2.62% at concentration sample 1.725 ppm in a cuvette while the lowest error was 0.47% at concentration 0.431 ppm in a 2.2 mm flow cell.

In a nutshell, 1 mm flow cell showed the lowest error compared to a 2.2 mm flow cell while a cuvette showed the largest error of the flow cell. In this case, the cylinder geometry form of the flow cell can reduce the error compared to the square geometry form of the cuvette.

Accuracy as showed in figure 20 that obtained by equation (10). Axis y started by 0.5 due to get detail difference for each sample cell.

$$acc(\bar{x}) = 1 - \frac{bias(\bar{x})}{\Delta\bar{x}} \tag{10}$$

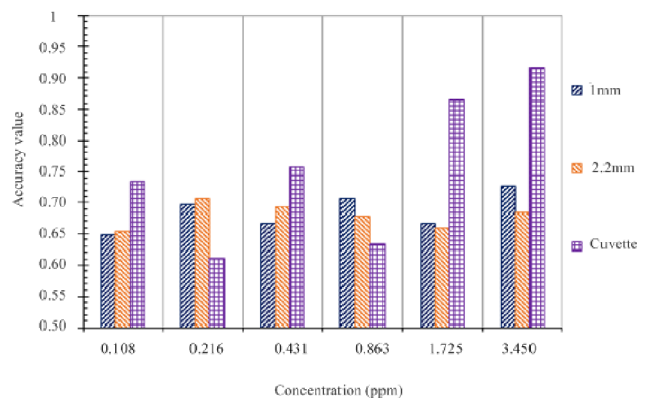


FIGURE 20. Accuracy.

The highest accuracy was 0.917 at concentration of 3.45 ppm and the lowest was 0.611 at 0.216 ppm concentration, both of which occur in cuvette. The mean value of accuracy was 0.685, 0.680, and 0.753 for sample 1 mm flow cell, 2.2 mm flow cell and the cuvette.

In the analysis of accuracy, the cuvette showed the highest mean of accuracy of 0.068 with variations 0.306 compare to 0.077 for a 1 mm flow cell and 0.051 flow cell for a 2.2 mm flow cell. It can be concluded that the flow cell has better stability than the cuvette.

**C. SENSITIVITY**

Sensitivity is a significant characteristic in any measurement process. In the viewpoint of instrumental measuring, sensitivity is defined as changes in the response of a measuring instrument divided by the corresponding change in analytic concentration [38].

Sensitivity of analytical procedure is defined as changes in measured value divided by the corresponding analytical value (concentration of analyte). In the case of linear calibration function, the sensitivity  $S_{AA}$  is determined by equation (11) as follow:

$$S_{AA} = \frac{\Delta y_A}{\Delta x_A} \tag{11}$$

Sensitivity data of the analysis is displayed in Figure 21. Sensitivity values are 0.3019, 0.3342, and 0.3099, for 1 mm flow cell, 2.2 mm flow cell, and cuvette, respectively.

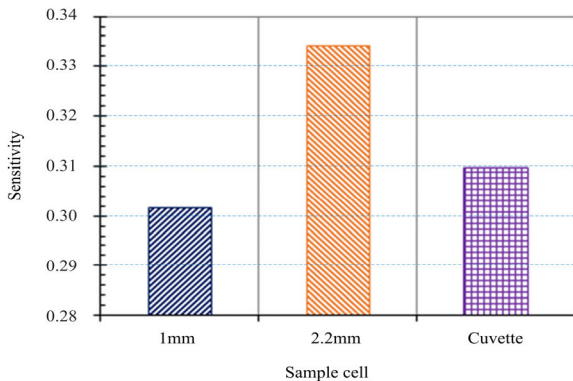


**FIGURE 21. Sensitivity.**

The highest sensitivity value was from the 2.2 mm flow cell, while the lowest was the 1 mm flow cell. The difference between the two was 0.024 for the 2.2 mm flow cell, which was higher than the 1 mm flow cell and 0.008 for the 1 mm flow cell compared to the cuvette.

Sensitivity of the 2.2 mm flow cell is the highest; while the lowest is the 1 mm flow cell. This phenomenon occurred due to the geometry effect. The larger cylinder diameter for the 2.2 mm flow cell allows a larger beam of light from the source to react with the sample.

**D. LIMIT OF DETECTION AND LIMIT OF QUANTITATION**

Limit of detection (LOD) and limit of quantification (LOQ) are the most important values for validation of analytical instruments [39].

LOD and LOQ are defined by calibration plot [40] as shown in equation (12) and (13):

$$LOD = \frac{3.3s}{m} \tag{12}$$

$$LOQ = \frac{10s}{m} \tag{13}$$

Table 2 shows LOD and LOQ values for the sample cells. The 1 mm flow cell shows the lowest LOD and LOQ, while the highest reading is given by the cuvette.

**TABLE 2. Limit of detection and limit of quantification.**

	Flow cell		Cuvette
	1 mm	2.2 mm	
<b>LOD</b>	0.07489	0.07573	0.07806
<b>LOQ</b>	0.24964	0.25242	0.26022

Table 2 shows that the smallest LOD and LOQ are from the 1-mm flow cell, which has the smallest volume. At low concentrations, the signal was still detected and this met the statistical standards. This occurs in a sample container with a smaller volume due to the light being focused onto the smaller sample cell.

**VIII. CONCLUSION**

A disposable flow cell design that is easily configured for assembly and discharged based on PMMA with aluminum casing has been demonstrated. POF was applied as for connector performed a linearity line in calibration analysis. The Calibration analysis with data control analysis showed there no data out of warning line. It has fulfilled the ISO 8285 standard. Data quality control is presented in box plot graph. The graphs showed that average value and data range are within warning line, it means the data met the standard.

Summary of comparison of the disposable flow cell designed and disposable cuvette showed in Table 3.

**TABLE 3. Summary of parameter comparison.**

Parameters	Flow cell		Cuvette
	1 mm	2.2 mm	
Validation of the mathematical model	3.676	4.226	4.715
Precision of an analytical procedure	0.966	0.964	0.967
Precision of an analytical result	0.704	0.760	0.753
Accuracy	0.685	0.680	0.753
Sensitivity	0.302	0.334	0.310

The table shows that differential data of parameter measurements are not significance. It means the design sample is acceptable compare to commercial sample cell.

## APPENDIX

### Limit of the one-sided F-Distribution

Limit of the one-sided F-Distribution

Limit of one-sided F-distribution for the significance level P = 95%													
df 1	2	3	4	5	6	7	8	9	10	12	20	∞	
1	161	199	216	225	230	234	237	239	241	242	244	6209	254
2	18.513	199.000	19.164	19.247	19.296	19.330	19.353	19.371	19.385	19.396	19.413	99.449	19.496
3	10.128	9.552	9.277	9.117	9.013	8.930	8.887	8.845	8.812	8.786	8.745	26.690	8.526
4	7.709	6.944	6.591	6.388	6.256	6.163	6.094	6.041	5.999	5.964	5.912	14.020	5.628
5	6.608	5.786	5.409	5.192	5.050	4.957	4.876	4.818	4.772	4.735	4.678	9.553	4.365
6	5.987	5.143	4.757	4.534	4.387	4.295	4.207	4.147	4.099	4.060	4.000	7.396	3.669
7	5.318	4.737	4.347	4.120	3.972	3.884	3.787	3.726	3.677	3.637	3.575	6.115	3.230
8	5.117	4.459	4.066	3.838	3.687	3.596	3.500	3.438	3.388	3.347	3.284	5.359	2.928
9	5.117	4.256	3.863	3.633	3.482	3.374	3.293	3.230	3.179	3.137	3.073	4.808	2.707
10	4.965	4.103	3.708	3.478	3.326	3.217	3.135	3.072	3.020	2.978	2.913	4.405	2.538
12	4.747	3.885	3.490	3.259	3.106	2.996	2.913	2.849	2.796	2.753	2.687	3.858	2.296
20	4.351	3.493	3.098	2.866	2.711	2.599	2.514	2.447	2.393	2.348	2.278	2.938	1.843
∞	3.841	2.605	2.605	2.372	2.214	2.099	2.010	1.938	1.880	1.831	1.752	1.878	1.008

From Excel function = FINV(5%, df1, df2)

Limit of one-sided F-distribution for the significance level P = 9%													
df 1	2	3	4	5	6	7	8	9	10	12	20	∞	
1	4.052	4.999	5.403	5.625	5.764	5.859	5.928	5.981	6.022	6.056	6.106	6.209	6.366
2	98.503	99.000	99.166	99.249	99.299	99.333	99.356	99.374	99.388	99.399	99.416	99.449	99.499
3	34.116	30.817	29.457	28.710	28.237	27.911	27.672	27.489	27.345	27.229	27.052	26.690	26.125
4	21.198	18.000	16.694	15.977	15.522	15.207	14.976	14.799	14.659	14.546	14.374	14.020	13.463
5	16.258	13.274	12.060	11.392	10.967	10.672	10.456	10.289	10.158	10.051	9.888	9.553	9.021
6	13.745	10.954	9.780	9.148	8.746	8.466	8.260	8.102	7.976	7.876	7.718	7.396	6.880
7	12.246	9.547	8.451	7.847	7.460	7.191	6.993	6.840	6.719	6.620	6.469	6.155	5.650
8	11.259	8.649	7.591	7.006	6.632	6.371	6.178	6.029	5.911	5.814	5.667	5.359	4.859
9	10.561	8.022	6.992	6.422	6.057	5.802	5.613	5.467	5.351	5.257	5.111	4.808	4.311
10	10.044	7.559	6.552	5.994	5.636	5.386	5.200	5.057	4.942	4.849	4.706	4.405	3.909
12	9.330	6.927	5.953	5.412	5.064	4.821	4.640	4.499	4.388	4.296	4.155	3.858	3.361
20	8.096	5.849	4.938	4.431	4.103	3.871	3.699	3.564	3.457	3.368	3.231	2.938	2.421
∞	6.635	4.605	3.782	3.319	3.017	2.802	2.639	2.511	2.407	2.321	2.185	1.878	1.011

From Excel function = FINV(1%, df1, df2)

## ACKNOWLEDGMENT

The authors are grateful to Ministry of Higher Education Malaysia, the Photonics Technology Laboratory, Center of Advanced Electronic and Communication Engineering (PAKET), Faculty of Engineering and Built Environment and the Center for Research and Instrumentation Management (CRIM), Universiti Kebangsaan Malaysia, for all the facilities provided.

## REFERENCES

[1] S. N. S. M. Zuki, N. S. Azmi, and T. L. Ling, "Mini review: Nitrite reductase and biosensors development," *Bioremediation Sci. Technol. Res.*, vol. 2, no. 2, pp. 5–9, 2014.

[2] R. Gürkan and N. Altunay, "Preconcentration and indirect quantification of trace nitrite, nitrate and total nitrite in selected beverage and milk samples using ion-pairing cloud-point extraction with acridine orange," *J. Food Compos. Anal.*, vol. 69, pp. 129–139, Jun. 2018.

[3] J. P. Schroeder, P. L. Croot, B. von Dewitz, U. Waller, and R. Hanel, "Potential and limitations of ozone for the removal of ammonia, nitrite, and yellow substances in marine recirculating aquaculture systems," *Aquacultural Eng.*, vol. 45, no. 1, pp. 35–41, 2011.

[4] D. Jalili, M. RadFard, H. Soleimani, S. Nabavi, H. Akbari, H. Akbari, A. Kavosi, A. Abasnia, and A. Adibzadeh, "Data on Nitrate–Nitrite pollution in the groundwater resources a Sonqor plain in Iran," *Data Brief*, vol. 20, pp. 394–401, 2018.

[5] M. Atta, W. Z. W. Yaacob, and O. B. Jaafar, "Steady state groundwater flow modeling of an ex-landfill site in Kuala Lumpur, Malaysia," *Amer. J. Environ. Sci.*, vol. 11, no. 5, pp. 348–357, May 2015.

[6] V. Rocher, A. M. Laverman, J. Gasperi, S. Azimi, S. Guérin, S. Mottelet, T. Villières, and A. Pauss, "Nitrite accumulation during denitrification depends on the carbon quality and quantity in wastewater treatment with biofilters," *Environ. Sci. Pollut. Res.*, vol. 22, no. 13, pp. 10179–10188, 2015.

[7] O. Mansour, M. Idris, N. M. Noor, M. S. B. Ruslan, and S. K. Das, "Effects of organic and commercial feed meals on water quality and growth of *Barbonymus schwanenfeldii* juvenile," *Aquaculture, Aquarium, Conservation Legislation*, vol. 10, no. 5, pp. 1037–1048, 2017.

[8] F. Gassara, A. P. Kouassi, S. K. Brar, and K. Belkacemi, "Green alternatives to nitrates and nitrites in meat-based products—A review," *Crit. Rev. Food Sci. Nutrition*, vol. 56, no. 13, pp. 2133–2148, 2016.

[9] Q.-H. Wang, L.-J. Yu, Y. Liu, L. Lin, R.-G. Lu, J.-P. Zhu, L. He, and Z.-L. Lu, "Methods for the detection and determination of nitrite and nitrate: A review," *Talanta*, vol. 165, pp. 709–720, Apr. 2017.

[10] N. A. Aljaber, B. R. Mhdi, S. K. Ahmmad, J. F. Hamode, M. M. Azzawi, A. H. Kalad, and S. M. Ali, "Design and construction fiber sensor detection system for water nitrite pollution," *IOSR J. Eng.*, vol. 4, no. 2, pp. 37–43, 2014.

[11] N. A. Cloete, R. Malekian, and L. Nair, "Design of smart sensors for real-time water quality monitoring," *IEEE Access*, vol. 4, pp. 3975–3990, 2016.

[12] P. Lindner, "Disposable sensor systems," in *Single-Use Technology in Biopharmaceutical Manufacture*. Hoboken, NJ, USA: Wiley, 2011, pp. 67–81.

[13] A. A. Shukla and U. Gottschalk, "Single-use disposable technologies for biopharmaceutical manufacturing," *Trends Biotechnol.*, vol. 31, no. 3, pp. 147–154, Mar. 2013.

[14] J. L. Novais, N. J. Titchener-Hooker, and M. Hoare, "Economic comparison between conventional and disposables-based technology for the production of biopharmaceuticals," *Biotechnol. Bioeng.*, vol. 75, no. 2, pp. 143–153, 2001.

[15] A. G. Lopes, "Single-use in the biopharmaceutical industry: A review of current technology impact, challenges and limitations," *Food Bioprod. Process.*, vol. 93, pp. 98–114, Jan. 2015.

[16] K. Higuchi and S. Motomizu, "Flow-injection spectrophotometric determination of nitrite and nitrate in biological samples," *Anal. Sci.*, vol. 15, no. 2, pp. 129–134, 1999.

[17] W. H. Wynn, "Inline optical sensor with modular flowcell," U.S. Patent 9279 746 B2, Feb. 16, 2012.

[18] D. L. Browne, S. Wright, B. J. Deadman, S. Dunnage, I. R. Baxendale, R. M. Turner, and S. V. Ley, "Continuous flow reaction monitoring using an on-line miniature mass spectrometer," *Rapid Commun. Mass Spectrometry*, vol. 26, no. 17, pp. 1999–2010, Sep. 2012.

[19] K. Lin, J. Ma, S.-C. Pai, Y. Huang, S. Feng, and D. Yuan, "Determination of nitrite, phosphate, and silicate by valveless continuous analysis with a bubble-free flow cell and spectrophotometric detection," *Anal. Lett.*, vol. 50, no. 3, pp. 510–529, Feb. 2017.

[20] S. Wang, K. Lin, N. Chen, D. Yuan, and J. Ma, "Automated determination of nitrate plus nitrite in aqueous samples with flow injection analysis using vanadium (III) chloride as reductant," *Talanta*, vol. 146, pp. 744–748, Jan. 2016.

[21] C. E. L. Pasquali, A. Gallego-Picó, P. F. Hernando, M. Velasco, and J. S. D. Alegría, "Two rapid and sensitive automated methods for the determination of nitrite and nitrate in soil samples," *Microchem. J.*, vol. 94, no. 1, pp. 79–82, Jan. 2010.

[22] C. G. Cooney, D. Sipes, N. Thakore, R. Holmberg, and P. Belgrader, "A plastic, disposable microfluidic flow cell for coupled on-chip PCR and microarray detection of infectious agents," *Biomed. Microdevices*, vol. 14, no. 1, pp. 45–53, 2012.

[23] S. Abubakar, N. Arsad, S. Nadia, M. S. Ab-Rahman, S. Shaari, A. A. Ehsan, and N. Arsad, "Polyethylene flow-injection for nitrite detection: Spectrophotometric method," in *Proc. 5th Int. Conf. Photon. (ICP)*, Sep. 2014, pp. 147–149.

[24] F. Abdurrahman, N. Arsad, S. Abubakar, and H. Ramza, "Simple design flow injection PMMA acrylic sample cell for nitrite determination," *Chin. Opt. Lett.*, vol. 12, no. 4, pp. 43002–43004, 2014.

[25] C. D. M. Campos and J. A. F. da Silva, "Applications of autonomous microfluidic systems in environmental monitoring," *RSC Adv.*, vol. 3, no. 40, pp. 18216–18227, 2013.

[26] C. H. Aparna and D. Gowrisankar, "A review on calibration of analytical instruments," *Int. J. Pharmaceutical, Chem. Biol. Sci.*, vol. 5, no. 3, pp. 573–582, 2015.

[27] F. A. Morrison, "Obtaining uncertainty measures on slope and intercept of a least squares fit with excel's LINEST," Dept. Chem. Eng., Michigan Technol. Univ., Houghton, MI, USA, 2015.

[28] M. Reichenbacher and J. W. Einax, "Performance verification of analytical instruments and tools: Selected examples," in *Challenges in Analytical Quality Assurance*. Berlin, Germany: Springer, 2011, pp. 269–285.

[29] O. Velychko and T. Gordiyenko, "The estimation of the measurement results with using statistical methods," *J. Phys., Conf. Ser.*, vol. 588, no. 1, Feb. 2015, Art. no. 012017.

[30] S. Abubakar, N. Arsad, M. S. Ab-Rahman, A. A. Ehsan, S. Shaari, and R. Othaman, "Study of geometrical effect of sample cell on nitrite determination," *J. Optoelectron. Adv. Mater.*, vol. 16, nos. 11–12, pp. 1487–1492, 2014.

[31] T. Guo, W.-H. Feng, X.-Q. Liu, H.-M. Gao, Z.-M. Wang, and L.-L. Gao, "Fourier transform mid-infrared spectroscopy (FT-MIR) combined with chemometrics for quantitative analysis of dextrin in Danshen (*Salvia miltiorrhiza*) granule," *J. Pharmaceutical Biomed. Anal.*, vol. 123, pp. 16–23, May 2016.

- [32] H. Juahir, S. M. Zain, M. K. Yusoff, T. I. T. Hanidza, A. S. M. Armi, M. E. Toriman, and M. Mokhtar, "Spatial water quality assessment of Langat River Basin (Malaysia) using environmetric techniques," *Environ. Monit. Assessment*, vol. 173, nos. 1–4, pp. 625–641, Feb. 2011.
- [33] M. Reichenbacher and J. W. Einax, "Solution to the quality assurance challenge 1," *Anal. Bioanal. Chem.*, vol. 383, no. 1, pp. 3–5, Sep. 2005.
- [34] A. C. Olivieri, "Analytical figures of merit: From univariate to multiway calibration," *Chem. Rev.*, vol. 114, no. 10, pp. 5358–5378, May 2014.
- [35] D. A. Skoog, F. J. Holler, and S. R. Crouch, *Principles of Instrumental Analysis*, 6th ed. San Francisco, CA, USA: Thomson Corporation, 2007.
- [36] K. Danzer, "Statistical evaluation of analytical results," in *Analytical Chemistry: Theoretical and Metrological Fundamentals*. Berlin, Germany: Springer, 2007, pp. 65–100.
- [37] K. Danzer, "Analytical performance characteristics," in *Analytical Chemistry*. Berlin, Germany: Springer, 2007, pp. 177–216.
- [38] W. Funk, V. Dammann, G. Donnevert, S. Ianelli, E. Ianelli, and A. Gray, "Phase I: Establishing a new analytical procedure," in *Quality Assurance in Analytical Chemistry*. Weinheim, Germany: Wiley, 2006, pp. 9–55.
- [39] N. Saadati, M. P. Abdullah, Z. Zakaria, S. B. T. Sany, M. Rezayi, and H. Hassonizadeh, "Limit of detection and limit of quantification development procedures for organochlorine pesticides analysis in water and sediment matrices," *Chem. Central J.*, vol. 7, no. 1, p. 63, Apr. 2013.
- [40] M. Belter, A. Sajnog, and D. Baralkiewicz, "Over a century of detection and quantification capabilities in analytical chemistry—Historical overview and trends," *Talanta*, vol. 129, pp. 606–616, Nov. 2014.



**ABANG ANNUAR EHSAN** received the B.E. degree in electrical engineering from UNSW, the M.Sc. degree in microelectronics from UKM, the M.Eng. degree in manufacturing system engineering from UPM, the Ph.D. degree in applied science from UiTM, and the Ph.D. degree in microengineering and nanoelectronics from UKM.

He is currently a Research Fellow with the Institute of Microengineering and Nanoelectronics (IMEN), Universiti Kebangsaan Malaysia. His research interests include optical design, photonics devices, and manufacturing processes for polymer and silicon devices.



**AZURA HAMZAH** received the B.S. degree in communication engineering from International Islamic University Malaysia, Malaysia, in 2005, and the M.S. degree in telecommunication engineering and the Ph.D. degree in fiber optic communications from the University of Malaya, Kuala Lumpur, Malaysia, in 2009 and 2012, respectively.

From 2011 to 2012, she was a Senior Lecturer with the Universiti Kuala Lumpur–British Malaysian Institute. Since 2013, she has been a Senior Lecturer with the Department of Electronic Systems Engineering, Malaysia-Japan International Institute of Technology, Universiti Teknologi Malaysia, Malaysia. Her research interests include fiber amplifier and laser, ultrashort pulse laser, optical interconnect, and optical sensors.

Dr. Azura Hamzah is one of the secretariats for the IEEE Photonics Society Malaysia Chapter.



**SABIRAN ABUBAKAR** received the B.Eng. degree in electronics engineering from Malikussaleh University, Indonesia, in 2006, and the M.S. degree in photonics engineering from UKM, Malaysia, in 2015. He is currently pursuing the Ph.D. degree in electronics systems engineering with the Malaysia-Japan International Institute of Technology (MJIIT), Universiti Teknologi Malaysia.

He was a Graduate Research Assistant with the Photonic Laboratory, Institute of Microengineering and Nanoelectronics. His research interests include imaging spectroscopy, spectroscopy, optical fiber sensor, biophotonics, and robotics.



**NUR HAZLIZA ARIFFIN** received the bachelor's degree in electronics engineering technology from the UniKL British Malaysian Institute, in 2008, and the M.Sc. degree in Microelectronics and the Ph.D. degree in electrical and electronics engineering from Universiti Kebangsaan Malaysia (UKM), in 2015 and 2019, respectively.

She has more than ten years of teaching experience. She was with UCSI University, from 2008 to 2015. She was a part-time Lecturer with Segi University, from 2017 to 2018. She is currently a Lecturer with the Department of Common Engineering, School of Engineering, Monash University Malaysia. Her research interests include the IoT, embedded systems, control systems, robotic design, and digital signal processing.



**NORHANA ARSAD** received the B.Eng. degree in computer and communication systems and the M.Sc. degree in photonics from Universiti Putra Malaysia (UPM), Malaysia, in 2000 and 2003, respectively, and the Ph.D. degree from the University of Strathclyde, Glasgow, U.K., in 2010.

She is currently an Associate Professor with the Center of Advanced Electronic and Communication Engineering, Faculty of Engineering and Built Environment, Universiti Kebangsaan Malaysia.

Her research interests include the investigation and design of fiber laser systems for application in spectroscopy, gas sensing, and photonics technology. She is also active in engineering education and entrepreneurial.



**MOHAMMAD SYUHAIMI AB-RAHMAN** received the B.Eng., M.Sc., and Ph.D. degrees in electrical, electronics, and systems engineering from Universiti Kebangsaan Malaysia (UKM), Bangi, Malaysia, in 2000, 2003, and 2007, respectively.

He is currently a Professor with the Department of electrical, Electronics, and System Engineering, Faculty of Engineering and Built Environment, UKM. He is also leading the Spectrum Technology Research Group, UKM. His research interests include optical communications system and photonic technology.

Prof. AB-Rahman is also a member of the Institute of Electronics, Information and Communication Engineers, Japan, The Institution of Engineers Malaysia, and the Board of Engineers Malaysia. He is also a Fellow of the Institute of Space Science.

• • •